Adv. Polar Upper Atmos. Res., **17**, 13–29, 2003

Characteristics of polar mesosphere summer echoes observed with oblique incidence HF radars at Syowa Station

Tadahiko Ogawa[1], Keisuke Hosokawa[2]*, Nozomu Nishitani[1], Natsuo Sato[3], Hisao Yamagishi[3] and Akira Sessai Yukimatu[3]

[1] *Solar-Terrestrial Environment Laboratory, Nagoya University, Honohara, Toyokawa 442-8507*
[2] *Department of Geophysics, Graduate School of Science, Kyoto University, Kyoto 606-8502*
[3] *National Institute of Polar Research, Kaga 1-chome, Itabashi-ku, Tokyo 173-8515*

(Received January 16, 2003; Accepted May 13, 2003)

Abstract: Polar mesosphere summer echoes (PMSE) are strong VHF–UHF radar echoes from the high-latitude cold mesopause at around 80–90 km altitudes in summer. Although a number of *in situ* and radar observations of PMSE have been made until now, generation mechanisms of PMSE and scattering processes of radar waves due to PMSE-associated irregularities are still controversial. In this paper, PMSE detected for the first time in December 1997 and January 1998 with the oblique incidence SuperDARN HF radars at Syowa Station, Antarctica (69.0°S, 39.6°E), are summarized to reveal the characteristics of PMSE at HF band. They appear at slant ranges of 180–315 km with elevation angles of 15°–30° between 1030 and 1230 UT or between 2100 and 0140 UT, and are characterized by durations of 65–110 min with intermittent subsidence and quasi-periodic oscillations of echo power with periods of 5–20 min, due to short-period atmospheric gravity waves. Detailed analysis of the December 15, 1997 event reveals the followings: 1) echo power is less than 30 dB, Doppler velocity between −40 and +40 m/s, and spectral width less than 50 m/s, respectively, 2) there exists no particular correlation among power, velocity and width, and 3) PMSE occurrence can be related to eastward neutral wind due to semi-diurnal tide that may induce the decrease in the mesospheric temperature.

key words: PMSE, Antarctic, neutral wind, gravity wave, HF radar

1. Introduction

Polar mesosphere summer echoes (PMSE), appearing at altitudes of 80–90 km in the high latitude mesosphere in summer, have been studied for twenty years or more by means of vertical incidence VHF–UHF radars in the Northern Hemisphere (see a review by Cho and Röttger, 1997 and references therein). Recently, Karashtin *et al.* (1997) and Kelley *et al.* (2002) have demonstrated the capability of vertical incidence HF systems for detecting PMSE at HF band. Thus, PMSE are a popular phenomenon at HF-UHF frequencies at northern high latitudes.

The knowledge of PMSE in the Southern Hemisphere, however, is very poor because of quite rare observation opportunities perhaps due to the warmer summer

* Now at Department of Information and Communication Engineering, University of Electro-Communications, Chofu-shi, Tokyo 182-8585.

mesopause at southern high latitudes (Balsley *et al.*, 1995; Huaman and Balsley, 1999) and/or a scarcity of radars suitable to PMSE observations. Woodman *et al.* (1999) have reported the first PMSE observations made in 1994 with a 50-MHz mesosphere-stratosphere-troposphere (MST) radar at a Peruvian base (62.1°S). Murphy and Vincent (2000) have noted enhanced echo amplitudes detected with a 1.94-MHz radar at Davis (68.6°S) that might be PMSE signatures at MF band. From *in situ* measurements of the mesosphere over Rothera (67.6°S), Lübken *et al.* (1999) have shown that the mesopause temperature in summer could become low ($\leq$140 K) enough to generate PMSE.

The Super Dual Auroral Radar Network (SuperDARN) HF radars at northern and southern high latitudes are equipped with oblique multiple beams to investigate the high latitude *E* and *F* region ionosphere (Greenwald *et al.*, 1995). These radars are also capable of measuring neutral winds in the upper mesosphere and lower thermosphere (80–100 km) by detecting meteor echoes (*e.g.*, Hall *et al.*, 1997; Yukimatu and Tutumi, 2002). Recently, Ogawa *et al.* (2002a) have detected, for the first time, peculiar upper mesosphere summer echoes at near ranges (180–315 km) with the SuperDARN HF radars at Syowa Station, Antarctica (69.0°S, 39.6°E). These echoes were clearly different from meteor echoes and were well explained by the PMSE hypothesis. Then, Ogawa *et al.* (2003) have compared upper mesosphere echoes, being very similar to the Syowa echoes, from the SuperDARN HF radar in Finland with PMSE simultaneously detected with an MST radar in Sweden. They have demonstrated that oblique incidence HF radars are surely suitable for the PMSE study.

In this paper, we analyze PMSE events observed with the Syowa HF radars in the austral summer of 1997–1998. Part of the current results have been published elsewhere (Ogawa *et al.*, 2002a). The main objectives of this paper are to summarize the detailed characteristics of PMSE at HF band that are not examined in the paper by Ogawa *et al.* (2002a) and to suggest a possible relation between PMSE occurrence and semi-diurnal neutral wind. Similarities and dissimilarities between PMSE at HF and VHF bands are briefly discussed.

2. Syowa HF radars

Figure 1 shows fields of view (FOVs) of two Syowa SuperDARN HF radars, called "Syowa South" and "Syowa East", in geographic coordinates. Each FOV is covered with 16 narrow beams (beam numbers 0, 1, 2, ..., 15; each beam width ~4.5°) over an azimuth sector of 52°. The beam directions of South beam 15 and East beam 0 are almost perpendicular to the magnetic *L*-shells. The radar frequency used in the current observations was around 11 MHz. At this frequency, as shown in Fig. 1, the radar beam in the vertical plane has maximum sensitivity at an elevation angle of about 30° with a half power beam width of 30°, being suitable for the detection of field-aligned *E* and *F* region irregularities at farther ranges (Greenwald *et al.*, 1985). The radar beam in the normal SuperDARN operation is sequentially scanned from beam 0 to beam 15 with a step in azimuth of around 3.3°, a scan repeat time of ~120 s, a range resolution of 45 km and a peak power of around 10 kW. The first range gate is set to 180 km.

Figure 1 also depicts contour lines (solid curves) of perpendicularity between the

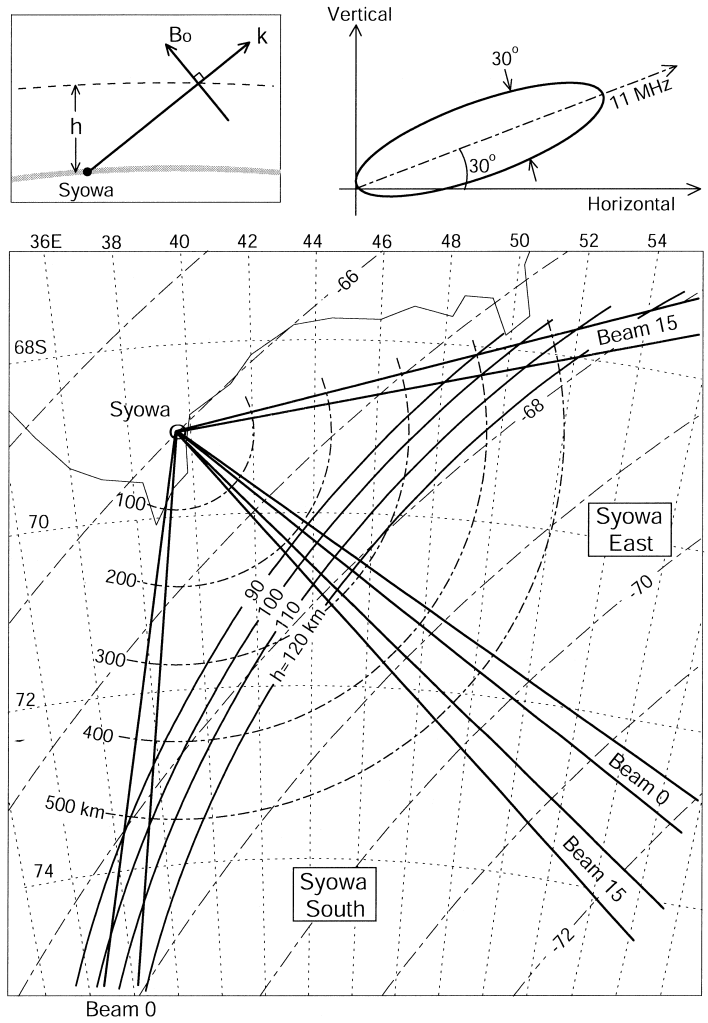

*Fig. 1. Fields of view of the Syowa South and East radars in geographic coordinates. Each FOV is covered with 16 narrow beams (beam numbers 0, 1, 2, ..., 15). Geomagnetic latitudes and ground ranges (100 km step) from Syowa Station are marked by the dot-dashed curves. Contour lines of perpendicularity between radar wave (**k**) and the geomagnetic field (B_0: IGRF95) vectors at altitudes of $h = 90$, 100, 110, and 120 km are shown by the solid curves. Schematic radar beam pattern at 11 MHz in the vertical plane is also depicted.*

radar wave vector and the geomagnetic field vector (IGRF95) at altitudes of $h = 90$, 100, 110, and 120 km. No radar wave refraction is assumed in the calculations. It is known that when wave refraction is weak, coherent echoes due to field-aligned *E* region irregularities are most strongly backscattered from the area covered by the four solid curves (Ogawa *et al.*, 2002b). Clearly, the *E* region echo ranges depend on radar beam number. To the contrary, as will be shown later, PMSE echo ranges do not depend on

the beam number and are close ($\leq$300 km) to Syowa Station on all the beams.

Echo power, Doppler velocity and spectral width are key parameters to represent echo characteristics. For the SuperDARN case, these parameters are deduced from an auto-correlation function (ACF) of radar echoes by assuming an exponential fit to ACF, which corresponds to a Lorentzian Doppler spectrum (*e.g.*, Hanuise *et al.*, 1993).

3. Observations

3.1. PMSE occurrence

Figure 2 displays slant range-time plots of the echo power observed on all the beams of the Syowa South and East radars on December 15, 1997. Part of the East radar echoes was discussed by Ogawa *et al.* (2002a). Signal to noise ratio (SNR) of the South radar was so high that the echoes with power exceeding 3 dB are plotted in the figure. The echoes occurred between 1130 and 1225 UT (UT=LT−3 hours; magnetic local time $\simeq$UT) for the South radar and between 1040 and 1230 UT for the East radar. Notice that some short-lived (2 min), range-isolated (45 km) echoes outside these intervals are due to meteors. For the East radar, the echoes exist mainly at ranges of 180–225 km (first range gate) and at some time intervals, at 180–315 km (first to third range gate). No meaningful echoes are detected at farther ranges beyond 315 km. For the South radar, although the echo ranges are similar to those for the East radar, the echo durations on all the beams are shorter than the South radar case, partly because of the poor SNR.

Time variation of the echo power maps from both radars between 1144 and 1214 UT is shown in Fig. 3. Notice that the weak echoes at ranges beyond 315 km ($\geq$fourth range gate) for the South radar are due to the high background noise. The echo powers are highly variable in space and time, indicating high spatial and temporal variabilities of the echo targets. Apparent movement of the strong echo region is southward on the East maps and eastward on the South maps. Such movements are also discernible in Fig. 2. Noteworthy is that vertical incidence HF-VHF radars can never provide such two-dimensional maps as shown in Fig. 3.

The fact that the echoes occur at the similar ranges on all the beams of both radars strongly indicates that they are not backscattered from *E* region irregularities: if they were *E* region echoes, the echo ranges would be dependent on the beam number, as Fig. 1 suggests. Ogawa *et al.* (2002b) have shown that when the ionosphere is highly disturbed, *E* region echo ranges become close to the radar site due to HF wave refraction caused by high energy particle precipitation. During 0900–1500 UT on December 15, 1997, 3-hour *K* indices at Syowa Station were 1 (geomagnetic disturbances of 25–50 nT) and K_p indices were 1 and 1-, again suggesting that our echoes are not echoes from field-aligned *E* region irregularities. Sporadic *E* (E_s) monitored by a routine ionosonde at Syowa Station was active on this day. The top frequencies of E_s, however, were always less than the radar frequency of 11 MHz, suggesting that our echoes are not originated from E_s reflection: see Ogawa *et al.* (2002a) for detailed discussion.

We looked for echoes, similar to those in Fig. 2, with the naked eye in the East radar data of June, July, December 1997 and January 1998, and selected echoes satisfying the following two conditions simultaneously: 1) geomagnetic conditions are

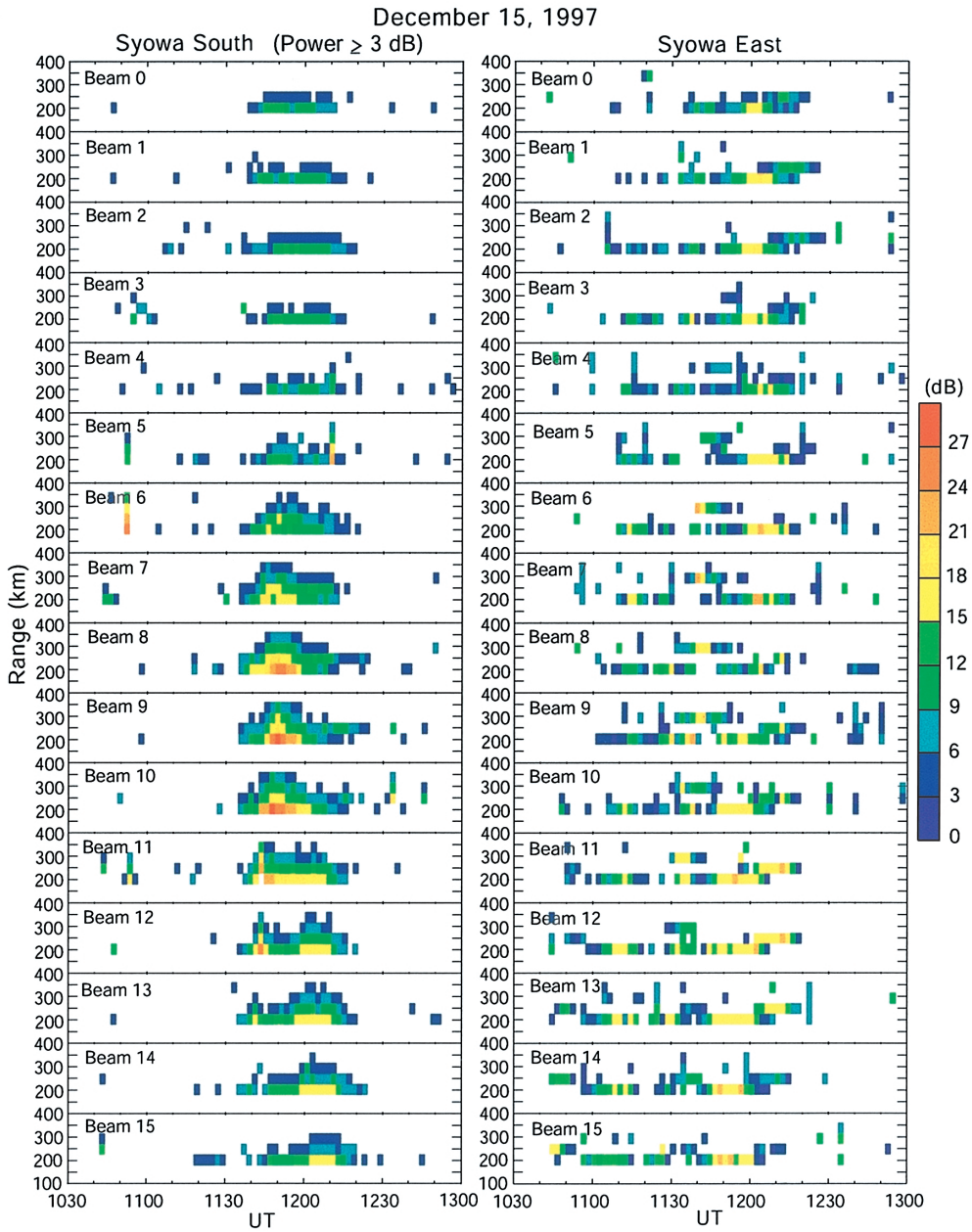

Fig. 2. Slant range-time plots of echo power on all beams of the Syowa South and East radars between 1030 and 1300 UT on December 15, 1997. Echoes with power exceeding 3 dB are shown for Syowa South.

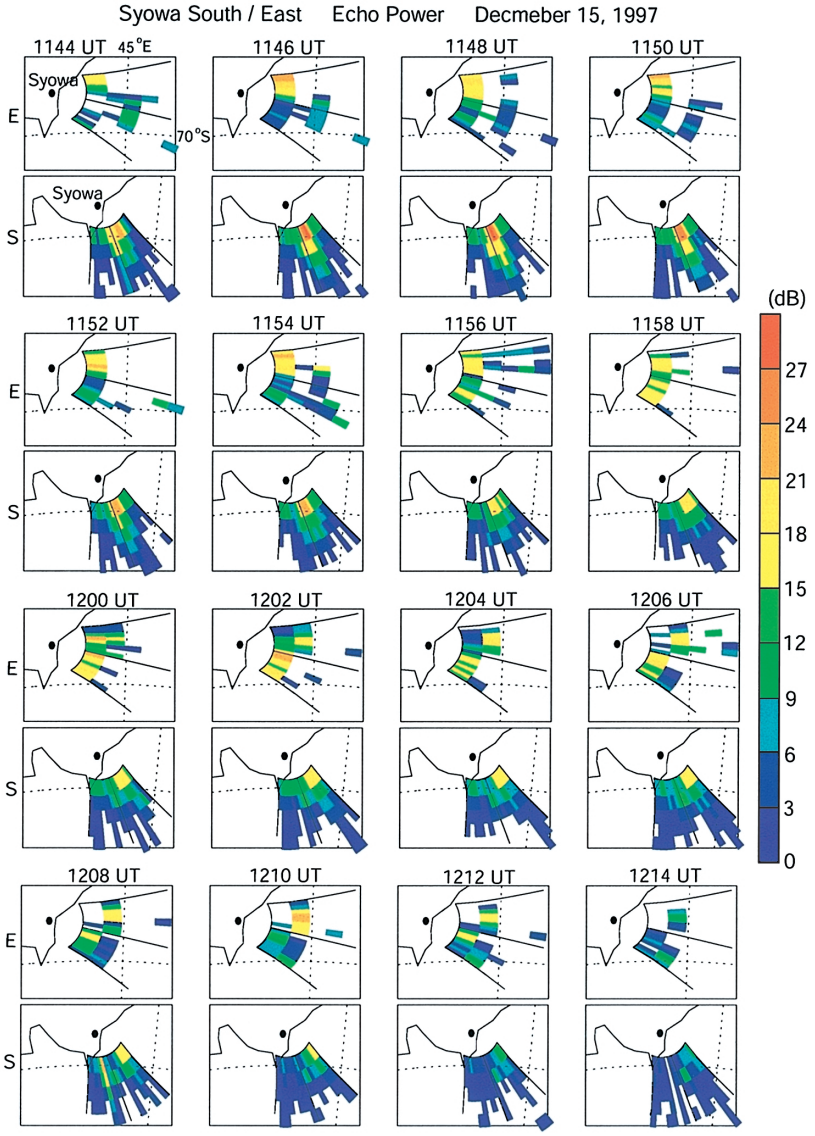

Fig. 3. Time variation of echo power maps (in geographic coordinates) from the Syowa South and East radars between 1144 and 1214 UT on December 15, 1997. Time goes from left to right and from top to bottom. First range gate and range resolution are 180 km and 45 km, respectively.

calm (Syowa K index=0 or 1) and 2) echoes, that exist somewhere between 180 and 315 km ranges and continue for more than 60 min with some intermittent subsidence, appear on almost all the radar beams. These criteria are sufficient to omit echoes from E region irregularities that become active for higher geomagnetic conditions. As a result, four events were identified. Notice that even if the echoes in which we are interested

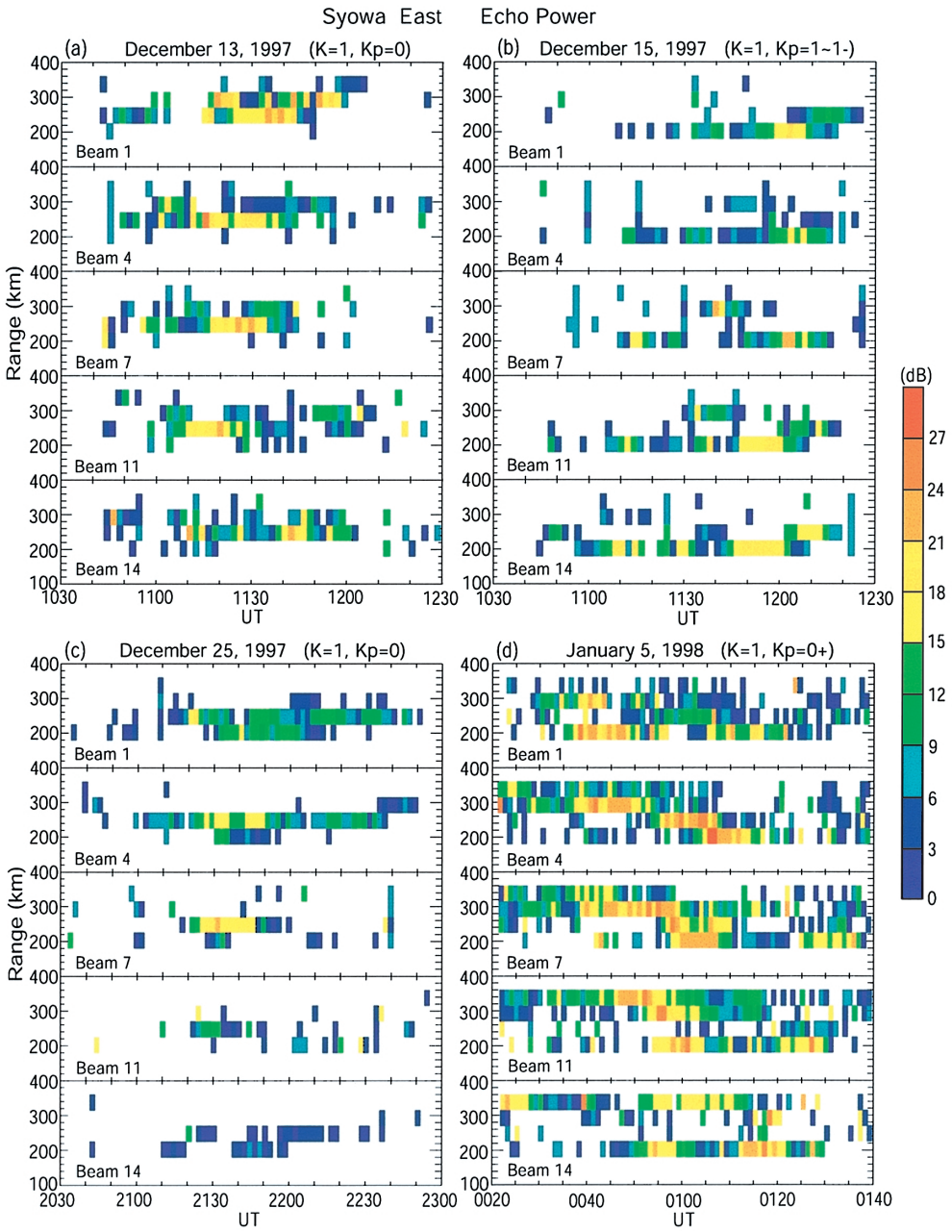

Fig. 4. Slant range-time plots of echo power on beams 1, 4, 7, 11, and 14 of the Syowa East radar on (a) December 13, 1997, (b) December 15, 1997, (c) December 25, 1997, and (d) January 5, 1998. Syowa K and K_p indices during echo occurrence are indicated.

appeared under disturbed geomagnetic conditions (say, $K \geq 2$), they were ignored because of possible contamination due to E region irregularities.

Figure 4 displays slant range-time plots of the echo power of the Syowa East radar for four events on December 13, December 15, December 25, 1997 and January 5, 1998. The December 15 case (Fig. 4b) has been discussed above in detail (Figs. 2 and 3). The other events appear at 225–315 km ranges during 1040–1210 UT on December 13 under $K=1$ and $K_p=0$ (Fig. 4a) and at 180–270 km ranges during 2100 and 2250 UT on December 25 under $K=1$ and $K_p=0$ (Fig. 4c). The January 5 event under $K=1$ and $K_p=0+$ (Fig. 4d) is a little complicated; though the echo appearance between 180 and 270 km during 0035–0140 UT are similar to that in other cases, the echoes beyond 270 km seem to originate from E irregularities because their ranges increase with increasing beam number. Notice that Syowa Station is under the auroral oval at around midnight. The Syowa South radar also detected similar echoes at 225–315 km during 1040–1150 UT on December 13 but it was not operative on December 25 and January 5. The events shown in Fig. 4 occurred only in summer and no events were identified in June and July 1997 (winter).

3.2. Doppler spectrum

Hereafter, PMSE observed on December 15, 1997 are analyzed in detail. In the SuperDARN operation, a seven-pulse sequence is used to determine a 17-lag ACF of backscattered signals (Greenwald *et al.*, 1985). As described above, echo power, Doppler velocity and spectral width are calculated from this ACF by assuming a Lorentzian Doppler spectrum. The ACF is Fourier-transformed into a 32-point Doppler spectrum with a spectral resolution of about 90 m/s. See a paper by Baker *et al.* (1995) for the detailed analysis of ACF.

Figure 5 shows Doppler spectra at the 180–225 km range gate during 1152–1206 UT on some beams of the Syowa South and East radars. Each spectrum is normalized by a maximum in the spectrum. Echo power P (dB), Doppler velocity V (m/s) and spectral width W (m/s) calculated from ACF are indicated in each spectrum. Notice that some spectra with zero and negative widths and with very low powers are not reliable: these are caused by wrong exponential fitting to ACF. Anyway, W's change a little with time and beam number. However, it is difficult to recognize this change from the spectra because the spectral resolution is 90 m/s and the abscissa covers from -1000 to $+1000$ m/s, which is suitable to the observations of E and F region plasma turbulence. We need sophisticated HF radar operation to get more detailed Doppler spectra of PMSE.

3.3. Relationship among echo power, Doppler velocity, and spectral width

Figure 6 shows time variations of P, V and W obtained at the 180–225 km range gate between 1050 and 1220 UT with the Syowa East radar. The following characteristics are found from this figure:

1) Radar echoes continue for about 80 min with intermittent subsidence.
2) Echo groups have durations of 5–30 min.
3) V, P, and W exhibit quasi-periodic oscillations with periods of 5–20 min.
4) V's are between -40 and $+10$ m/s but mostly negative, meaning that the scatterers

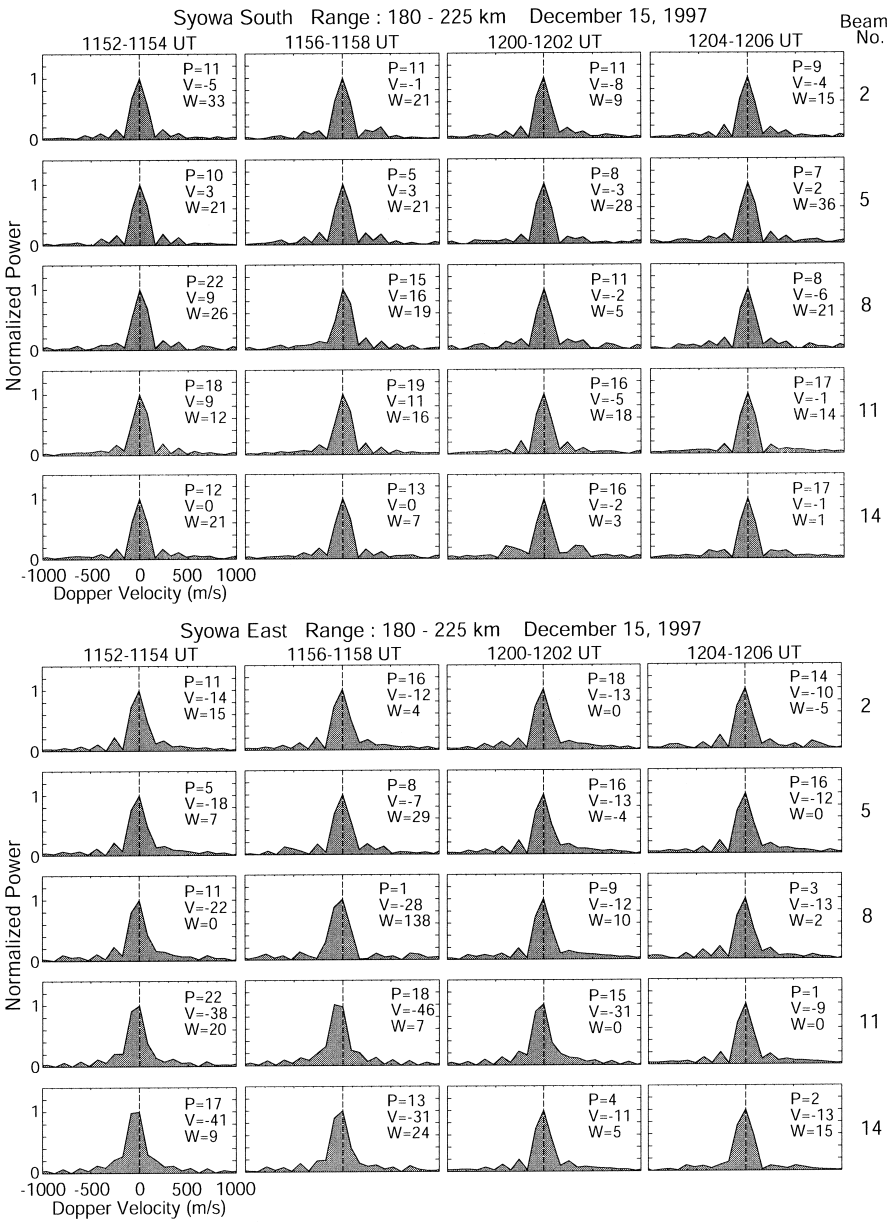

Fig. 5. Normalized Doppler spectra obtained at 180–225 km range gate on some beams of the Syowa South and East radars during 1152–1206 UT on December 15, 1997. Echo power (P in dB), Doppler velocity (V in m/s), and spectral width (W in m/s) calculated from auto-correlation function are indicated in each spectrum.

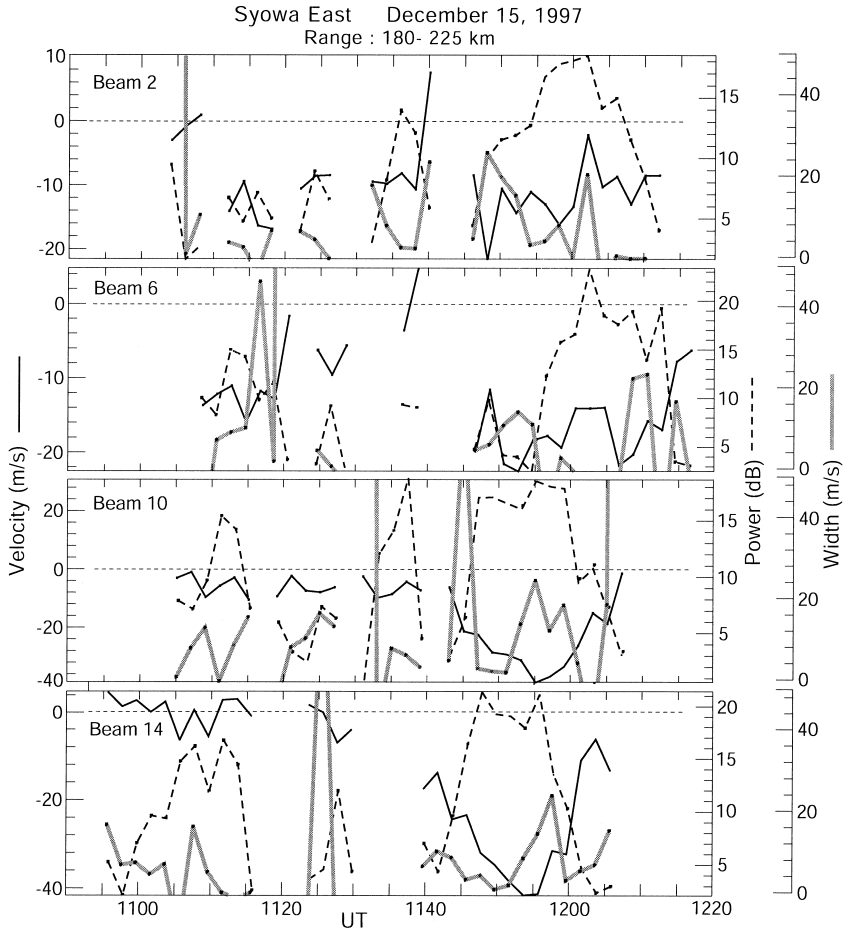

Fig. 6. Time variations of Doppler velocity, echo power, and spectral width obtained at 180–225 km range gate with the Syowa East radar on December 15, 1997.

move away from the radar. P's are less than 25 dB. W's are mostly less than 30 m/s.

5) No particular correlation exists among P, V, and W.

Röttger (1994) summarized important features of the Arctic PMSE that were observed with vertical incidence VHF radars (range resolution $\leq$1 km) as follows: i) PMSE exist at altitudes between 80 and 89 km, preferably at 82–86 km, ii) scatter amplitudes are highly variable with typical temporal scales of 10 s to 5–20 min and their variations are almost not correlated between adjacent range gates that are separated by 1 km, iii) vertical velocities oscillate up to $\pm$5 m/s with periods of 6–15 min, iv) echo amplitude variability is not clearly related to certain phases of velocity oscillations, and v) spectral width are extremely narrow but also large. Although our HF radars have oblique beams and quite poor range resolution (45 km), items ii, iii, iv and v are very consistent with the above items 2, 3, and 5.

Figure 7 displays scatter plots between W and P, V and P, and V and W for the

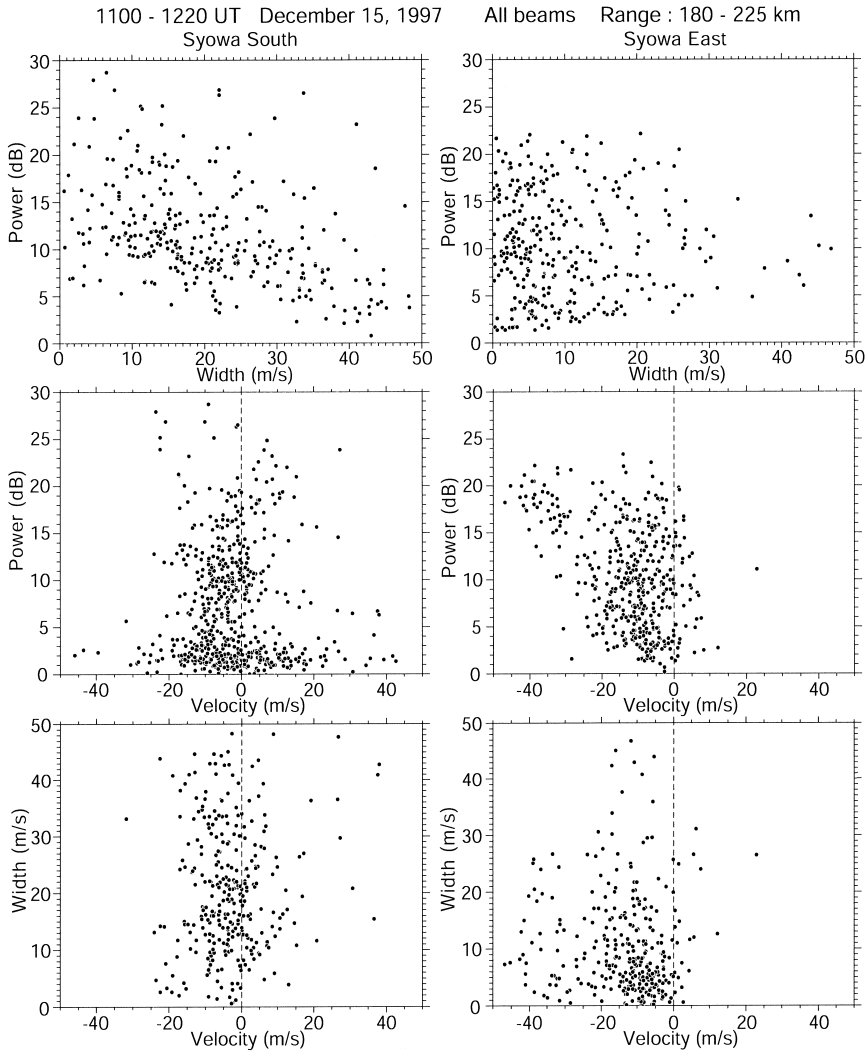

Fig. 7. Scatter plots between (top) W and P, (middle) V and P, and (bottom) V and W for (left) the Syowa South and (right) East radars. To make these plots, data at 180–225 km range gate on all beams during 1100–1220 UT on December 15, 1997 are used.

South and East radars. To make these plots, we utilized all the P, V, and W data at the 180–225 km range gate during 1100–1220 UT. For the South radar, P, V and W are less than 30 dB, between -20 and $+40$ m/s, and less than 50 m/s, respectively (notice that the data with V less than -25 m/s in the V-P plot have W's beyond 50 m/s). Those for the East radar are less than 25 dB, between -40 and $+10$ m/s, and mostly less than 40 m/s, respectively. There exist no general correlations among P, V, and W, although a weak correspondence between V and P is discernible for the East data. P seems to decrease with increasing W for the Syowa South data (Arnold *et al.*, 2001).

The magnitudes of V shown in Fig. 7 are consistent with neutral wind velocities in the upper mesosphere and lower thermosphere over Syowa Station (Ogawa *et al.*, 1985; Tsutsumi *et al.*, 2001; Yukimatu and Tsutsumi, 2002), meaning that the scatterers move with neutral winds. Clearly, their temporal and spatial variations are attributable to short-period atmospheric gravity waves (*e.g.*, Williams *et al.*, 1989; Rüster *et al.*, 1996).

3.4. Spatial variations of echo power and Doppler velocity

Doppler velocities from both radars are combined to see two-dimensional movement of the scatterers. Figure 8 shows variations of V and P at the 180–225 km range gate as a function of the beam number at 1152, 1156, 1200, and 1204 UT. For the South radar, V's are less than $\pm$10 m/s and positive before 1200 UT but negative after that. For the East radar, V's are much larger than those of the South radar and have maximums on beams 11–13 that are directed eastward (Fig. 1). Considering the time variations of V's from both radars and the FOVs in Fig. 1 tells that the scatterers moved, as a whole, east-northeastward before 1200 UT and eastward after that. This eastward movement is confirmed in the P plot for the Syowa South; that is, the strongest echo region moves clearly eastward with time.

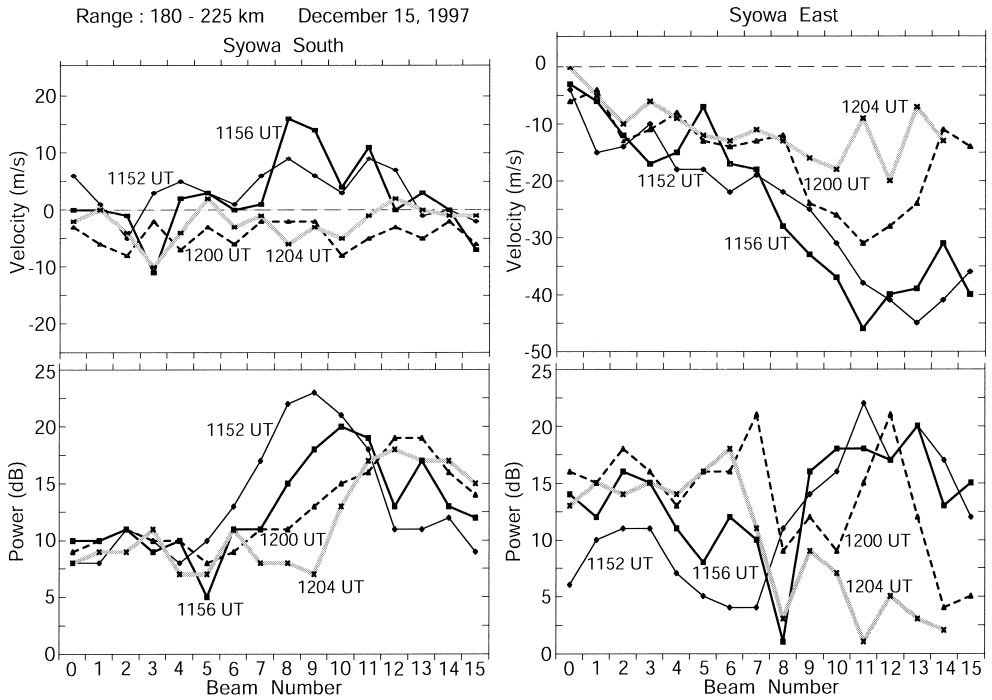

Fig. 8. Variations of Doppler velocity and echo power at 180–25 km range gate as a function of beam number for (left) the Syowa South and (right) East radars at 1152, 1156, 1200 and 1204 UT on December 15, 1997.

4. Discussion

Until now, PMSE have been observed using vertical pointing beams because PMSE are strongest for the vertical beam with a very high aspect sensitivity; that is, scattering is much higher in the vertical direction than from off-vertical. From VHF radar observations, Czechowsky *et al.* (1988) found highly aspect-sensitive echoes in the main vertical beam and non aspect-sensitive echoes with two grating lobes at elevations of 52° and 55°. They suggested that there was a transition from dominant quasi-specular to more isotropic backscattering with increasing off-zenith angle. Our HF PMSE, however, were detected at ranges of 180–315 km. How can we account for this fact? Figure 9 gives a schematic illustration to explain the observational results. As shown in Fig. 1, the radar beam pattern in the vertical plane has maximum sensitivity at an elevation angle of about 30° with a half power beam width of 30°, and the sensitivity at angles larger than 60° is believed to be very low. The first range gate is 180 km and the range resolution is 45 km. In this situation, when horizontally-extended turbulence causing backscatter exists at 80–90 km altitudes, the radar can detect echoes only at ranges of 180–315 km. The fact that PMSE are observed at low elevation angles between 15° and

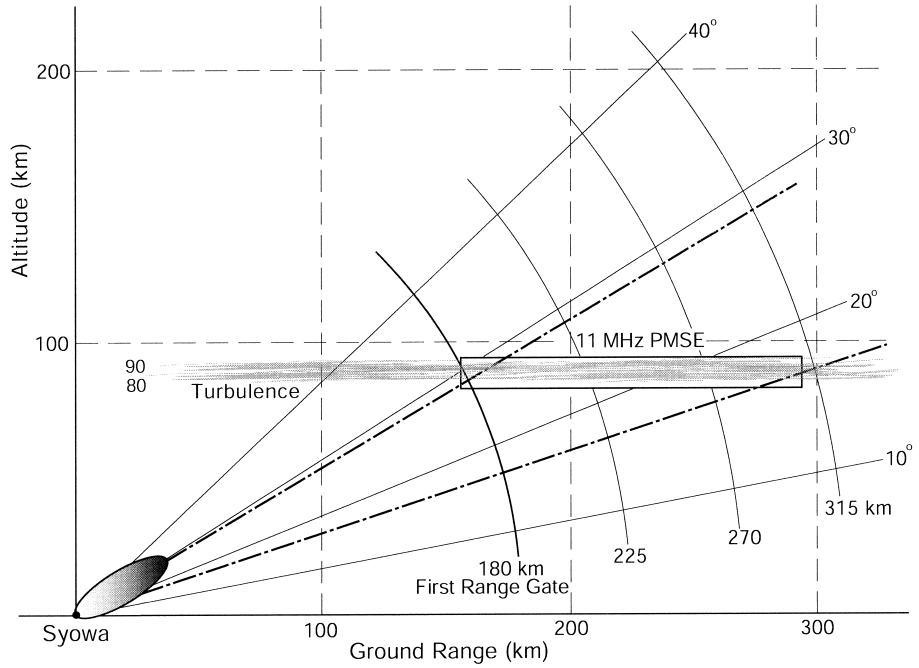

Fig. 9. Schematic illustration to explain PMSE detected with the Syowa 11 MHz HF radar. The radar beam in the vertical plane has maximum sensitivity at an elevation angle of about 30° with a half power beam width of 30°. The first range gate and range resolution are 180 and 45 km, respectively. When horizontally-extended turbulence exists at 80–90 km altitudes, the radar can detect echoes only at ranges of 180–315 km.

30° suggests that the scattering targets seen by the HF radar have no severe aspect sensitivity and are rather "isotropic".

Most theories to explain the generation of PMSE at around 50 MHz (Bragg wavelength of 3 m) rely on enhancement of 3-m scale fluctuation embedded in neutral air turbulence (*e.g.*, Cho and Röttger, 1997). However, the 3-m fluctuation amplitude within normal air turbulence is not enough to invoke radar backscattering; that is, a scale of 3 m is far smaller than the inertial cutoff length of the turbulence. It is now believed that the backscattering becomes possible when large aerosols or ice particles that deduce effectively the electron diffusivity are generated in the cold mesopause to enhance the 3-m fluctuations. Such a situation is also applicable to the 11-MHz PMSE (Bragg wavelength of 14 m) when a scale of 14 m is outside the inertial cutoff length. However, question of whether this scale is already inside the inertial subrange or not remains to be resolved. Moreover, we do not know why our HF PMSE are detected at low elevations angles where VHF PMSE have never been found.

Ogawa *et al.* (2003), who have reported PMSE simultaneously detected at four frequencies of 9, 11, 13 and 15 MHz with the CUTLASS Finland HF radar (first range gate=80 km and range resolution=15 km), one of the SuperDARN radars, find that echo ranges are 105–250 km at 9 and 11 MHz while they are 105–135 km at 13 and 15 MHz, and echo power decreases with increasing frequency. To explain these characteristics, the following factors must be taken into account: wavenumber spectrum of radar reflectivity, aspect sensitivity of scatterers and instrumental effect (*e.g.*, antenna gain pattern in the vertical plane). These factors depend on radar frequency. Current PMSE at 11 MHz must be understood in this context. Surely, simultaneous PMSE observations with vertical and oblique beams are highly required to explore the generation mechanism of PMSE at HF band.

In Fig. 4, the timings of PMSE occurrence on December 13 (Fig. 4a) and 15 (Fig. 4b) differ, by about 12 hours, from those on December 25 (Fig. 4c) and January 5 (Fig. 4d), suggesting that the occurrence is controlled by semi-diurnal tides. Palmer *et al.* (1996) showed that PMSE observed with the EISCAT VHF radar appear most frequently around noon and midnight, which is fairly consistent with our results. Williams *et al.* (1995) pointed out that PMSE occurrence is closely related to the phase of semi-diurnal tide. The eastward neutral wind, with which scatterers causing PMSE move, derived from Doppler velocity data of two Syowa HF radars (Fig. 8), might be due to semi-diurnal tide. Thus, the PMSE occurrence can be related to the decrease of the mesospheric temperature induced by semi-diurnal tides (*e.g.*, Rüster, 1995).

5. Summary

Four PMSE events were detected for the first time in the summer of 1997–1998 with the Syowa South and/or East HF radars. Their characteristics are summarized as follows:

1) PMSE are observed at slant ranges of 180 (first range gate)–315 km. This fact is quite reasonable when the main antenna beam with an elevation of about 30° (half power beam width of 30°) is considered, and indicates that scatterers causing PMSE have no severe aspect sensitivity.

2) They appear between 1030 and 1230 UT or between 2100 and 0140 UT. These timings are consistent with past PMSE observations with the EISCAT VHF radar.
3) They are characterized by durations of 65–110 min with intermittent subsidence and quasi-periodic oscillations of echo power with periods of 5–20 min, due to short-period atmospheric gravity waves.

Detailed analysis of the December 15, 1997 event indicates:

4) Echo power, Doppler velocity and spectral width are less than 30 dB, between −20 and +40 m/s and less than 50 m/s, respectively, for the South radar, and are less than 25 dB, between −40 and +10 m/s and mostly less than 40 m/s, respectively, for the East radar.
5) When PMSE appeared, neutral wind (perhaps due to semi-diurnal tide) was eastward.

The above items 1–4 are support the Syowa results (Ogawa *et al.*, 2002a) and also applicable to the Arctic PMSE at HF band (Ogawa *et al.*, 2003). As to item 5, in the future, simultaneous PMSE and neutral wind observations are highly required to disclose the relationship between PMSE occurrence and neutral wind behavior.

PMSE have been extensively studied using Arctic VHF radars. However, the generation and scattering processes of PMSE at HF band remain to be resolved. At this stage, we are not sure whether these processes can be explained within a framework of PMSE at VHF band or not. Many SuperDARN radars have been routinely working to observe the northern and southern high latitude ionosphere. We believe that these radars also provide data that are useful for exploring PMSE occurrences in both hemispheres.

Acknowledgments

We thank all the staff who contributed to the HF radar operation at Syowa Station. This research is supported by the Grant-in Aid for Scientific Research (A: 11304029) from Japan Society for the Promotion of Science (JSPS). The Ministry of Education, Culture, Sports, Science and Technology supports the Syowa HF radar system.

The editor thanks Dr. Cesar La Hoz and another referee for their help in evaluating this paper.

References

Arnold, N.F., Robinson, T.R., Lester, M., Byrne, P.B. and Chapman, P.J. (2001): Super Dual Auroral Radar Network observations of fluctuations in the spectral distribution of near range meteor echoes in the upper mesosphere and lower thermosphere. Ann. Geophys., **19**, 425–434.

Baker. K.B., Dudeney, J.R., Greenwald, R.A., Pinnock, M., Newell, P.T., Rodger, A.S., Mattin, N. and Meng, C.-I. (1995): HF radar signatures of the cusp and low-latitude boundary layer. J. Geophys. Res., **100**, 7671–7695.

Balsley, B.B., Woodman, R.F., Sarango, M., Rodriguez, R., Urbina, J., Ragaini, E., Carey, J., Huaman M. and Giraldez, A. (1995): On the lack of southern hemisphere polar mesosphere summer echoes. J. Geophys. Res., **100**, 11685–11693.

Cho, J.Y.N. and Röttger, J. (1997): An updated review of polar mesosphere summer echoes: Observation, theory, and their relationship to noctilucent clouds and subvisible aerosols. J. Geophys. Res., **102**, 2001–2020.

Czechowsky, P., Reid, I.M. and Ruster, R. (1988): VHF radar measurements of the aspect sensitivity of the summer polar mesopause echoes over Andenes (69°N, 16°E), Norway. Geophys. Res. Lett., **15**, 1259–1262.

Greenwald, R.A., Baker, K.B., Hutchins, R.A. and Hanuise, C. (1985): An HF phased-array radar for studying small-scale structure in the high-latitude ionosphere. Radio Sci., **20**, 63–79.

Greenwald, R.A., Baker, K.B., Dudeney, J.R., Pinnock, M., Jones, T.B., Thomas, E.C., Villain, J.-P., Cerisier, J.-C., Senior, C., Hanuise, C., Hunsucker, R.D., Sofko, G., Koehler, J., Nielsen, E., Pellinen, R., Walker, A.D.M., Sato, N. and Yamagishi, H. (1995): DARN/SuperDARN: A global view of the dynamics of high-latitude convection. Space Sci. Rev., **71**, 761–796.

Hall, G.E., MacDougall, J.W., Moorcroft, D.R., St.-Maurice, J.-P., Manson, A.H. and Meek, C.E. (1997): Super Dual Auroral Radar Network observations of meteor echoes. J. Geophys. Res., **102**, 14603–14614.

Hanuise, C., Villain, J.P., Gresillon, D., Cabrit, B., Greenwald, R.A. and Baker, K.B. (1993): Interpretation of HF radar ionospheric Doppler spectra by collective wave scattering theory. Ann. Geophys., **11**, 29–39.

Huaman, M.M. and Balsley, B.B. (1999): Differences in near-mesopause summer winds, temperatures, and water vapor at northern and southern latitudes as possible causal factors for inter-hemispheric PMSE differences. Geophys. Res. Lett., **26**, 1529–1532.

Karashtin, A.N., Shlyugaev, Yu.V., Abramov, V.I., Belov, I.F., Berezin, I.V., Bychkov, V.V., Eryshev, E.B. and Komrakov, G.P. (1997): First HF radar measurements of summer mesopause echoes at SURA. Ann. Geophys., **15**, 935–941.

Kelley, M.C., Huaman, M.M., Chen, C.Y., Ramos, C., Djuth, F. and Kennedy, E. (2002): Polar mesosphere summer echo observations at HF frequencies using the HAARP Gakona Ionospheric Observatory. Geophys. Res. Lett., **29** (12), 10.1029/2001GL013411.

Lübken, F.-J., Jarvis, M.J. and Jones, G.L.O. (1999): First in situ temperature measurements at the Antarctic summer mesopause. Geophys. Res. Lett., **26**, 3581–3584.

Murphy, D.J. and Vincent, R.A. (2000): Amplitude enhancements in Antarctic MF radar echoes. J. Geophys. Res., **105**, 26683–26693.

Ogawa, T., Igarashi, K., Kuratani, Y., Fujii, R. and Hirasawa, T. (1985): Some initial results of 50 MHz meteor radar observation at Syowa Station. Mem. Natl Inst. Polar Res., Spec. Issue, **36**, 254–263.

Ogawa, T., Nishitani, N., Sato, N., Yamagishi, H. and Yukimatu, A.S. (2002a): Upper mesosphere summer echoes detected with the Antarctic Syowa HF radar. Geophys. Res. Lett., **29** (7), 10.1029/2001GL014094.

Ogawa, T., Nishitani, N., Sato, N., Yamagishi, H. and Yukimatu, A.S. (2002b): *E* region echoes observed with the Syowa HF radar under disturbed geomagnetic conditions. Adv. Polar Upper Atmos. Res., **16**, 84–98.

Ogawa, T., Arnold, N.F., Kirkwood, S., Nishitani, N. and Lester, M. (2003): Finland HF and Esrange MST radar observations of polar mesosphere summer echoes. Ann. Geophys., **21**, 1047–1055.

Palmer, J.R., Rishbeth, H., Jones, G.L.O. and Williams, P.J.W. (1996): A statistical study of polar mesosphere summer echoes observed by EISCAT. J. Atmos. Terr. Phys., **58**, 307–315.

Röttger, J. (1994): Polar mesosphere summer echoes: Dynamics and aeronomy of the mesosphere. Adv. Space Res., **14**, (9) 123–(9)137.

Rüster, R. (1995): Velocity and associated echo power variations in the summer polar mesosphere. Geophys. Res. Lett., **22**, 65–67.

Rüster, R., Czechowsky, P., Hoffmann, P. and Singer, W. (1996): Gravity wave signatures at mesospheric heights. Ann. Geophys., **14**, 1186–1191.

Tsutsumi, M., Aso, T. and Ejiri, M. (2001): Initial results of Syowa MF radar observations in Antarctica. Adv. Polar Upper Atmos. Res., **15**, 103–116.

Williams, P.J.S., van Eyken, A.P., Hall, C. and Röttger, J. (1989): Modulation in the polar mesosphere summer echoes and associated with atmospheric gravity waves. Geophys. Res. Lett., **16**, 1437–1440.

Williams, P.J.S., Jones, G.O.L., Palmer, J.R. and Rishbeth, H. (1995): The association of polar mesosphere summer echo layers with tidal modes. Ann. Geophys., **13**, 454–457.

Woodman R.F., Balsley, B.B., Aquino, F., Flores, L., Vazquez, E., Sarango, M., Huaman, M.M. and Soldi,

H. (1999): First observations of polar mesosphere summer echoes in Antarctica. J. Geophys. Res., **104**, 22577–22590.

Yukimatu, A.S. and Tsutsumi, M. (2002): A new SuperDARN meteor wind measurement: Raw time series analysis method and its application to mesopause region dynamics. Geophys. Res. Lett., **29** (20), 1981, doi: 10.1029/2002GL015210; also see Correction, Yukimatu, A.S. and Tsutsumi, M. (2003), Geophys. Res. Lett., **30** (1), 1026, doi: 10.1029/2002GL016560.